DEPARTMENT OF PHYSICS

Master degree in Physics

Chaotic dynamics of an electronic implementation of the Burridge-Knopoff model

Graduant:
Manuel BITTO

Supervisor:
Leonardo RICCI

Co-supervisor:
Alessio PERINELLI

24 October 2024

Contents

Introduction

Chapter 1

An electronic analog of the Burridge-Knopoff model

1.1 Mechanical Burridge-Knopoff model

The Burridge-Knopoff (BK) spring-block model [1] is a two-dimensional system of massive blocks lying on a rough horizontal surface. Each block is connected to its nearest neighbors by a set of springs, and linked through another spring to an upper horizontal ceiling moving with constant velocity with respect to the lower plate, as shown in Fig. 1.1.

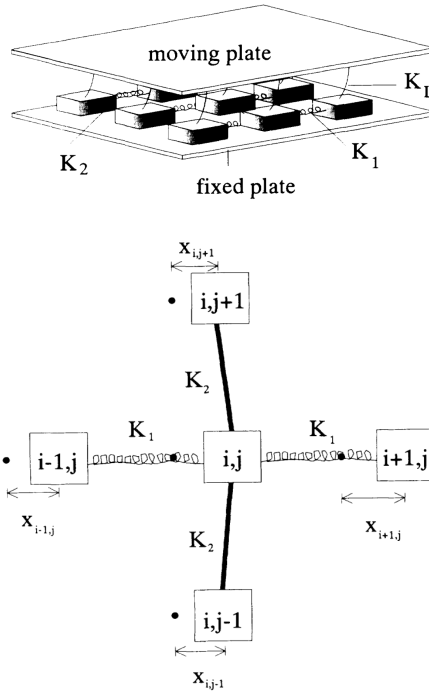Figure 1.1: Visual representation of the Burridge-Knopoff spring-block model. K_1 and K_2 are the elastic constants, respectively, of the horizontal and vertical springs, while K_L is the elastic constant of the springs connecting the blocks and the moving plate. The figure below represents the interaction between a block and its four nearest neighbors, as a function of the displacement $x_{i,j}$. Figure adapted from Ref. [2].

The blocks are driven by the relative movement of the two rigid plates. When the force on one block reaches some threshold value F_{th}, the block slips, and it is reasonable to assume that the force on that block becomes zero. Then, the force on the four nearest neighbors is increased, often resulting in further slips, and an avalanche can occur.

The purpose of the BK model is the description of the dynamical behavior of real faults, whereby a constant, slow driving motion of plates produces an accumulation of "stress" up to a threshold at which such stress is released through an abrupt motion − i.e., an earthquake − of one or more of the system's constituent parts.

1.1.1   Motion of two coupled blocks

The mechanical BK model for the motion of two coupled blocks is shown schematically in Fig. 1.2. The upper ceiling moves with respect to the surface with a constant velocity u_d. Let x_1, x_2 be the displacements of the block positions relative to a state in which the springs are relaxed, and u_1, u_2 the velocities of the blocks in the lower surface frame, so that $u_i = u_d + \dot{x}_i$ with $i = 1, 2$.
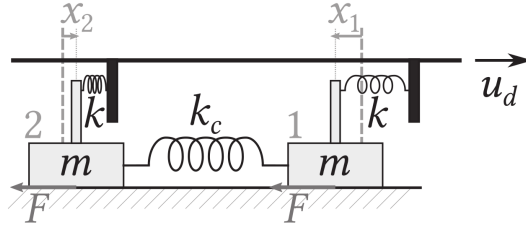

Figure 1.2: Two-blocks mechanical BK model. The upper ceiling, which the blocks are coupled to via springs with elastic constant k, is dragged with constant velocity u_d with respect to the underlying surface. This surface exerts a nonlinear, velocity-dependent friction F to each block's motion. Figure adapted from Ref. [3].

The equations of motion are thus given by

$$m\frac{\mathrm{d}u_1}{\mathrm{d}t} = -kx_1 - k_c(x_1 - x_2) - F(u_1),$$

$$\frac{\mathrm{d}x_1}{\mathrm{d}t} = u_1 - u_d,$$

$$m\frac{\mathrm{d}u_2}{\mathrm{d}t} = -kx_2 - k_c(x_2 - x_1) - F(u_2),$$

$$\frac{\mathrm{d}x_2}{\mathrm{d}t} = u_2 - u_d,$$

(1.1)

where m is the mass of the blocks, k is the elastic constant of the springs that connect the blocks to the ceiling, k_c is the elastic constant of the spring linking the two blocks, and $F(u)$ is the nonlinear velocity-dependent friction. The velocities are assumed to be non-negative.

1.1.2 Dimensionless system

It is possible to render this system dimensionless by defining the following dimensionless quantities (i takes the values 1 and 2): a time $\tau \equiv t\sqrt{k/m}$, a velocity $\nu_i \equiv u_i/u_0$, a position $\xi_i \equiv x_i\sqrt{k/m}/u_0$, a friction $\varphi(\nu_i) \equiv F(\nu_i)/(u_0\sqrt{mk})$ and a parameter $\lambda \equiv k_c/k$. The four equations of motion can then be written as

$$\frac{d\nu_i}{d\tau} = -(1+\lambda)\xi_i + \lambda\xi_{3-i} - \varphi(\nu_i),$$
$$\frac{d\xi_i}{d\tau} = \nu_i - \nu_d. \tag{1.2}$$

There exists a relative freedom in the choice of the friction $\varphi(\nu)$, provided that (i) $\varphi(\nu < 0) = 0$, (ii) $\varphi(\nu \geq 0) \geq 0$ and (iii) $\varphi(\nu)$ decreases down to zero from a maximum value $\varphi(0)$ that occurs at $\nu = 0$.

It is useful to define the equations of motion also in the case of a lower surface moving with a positive dimensionless velocity $\Delta\nu$, so that $\nu_i' = \nu_i + \Delta\nu$ and $\nu_d' = \nu_d + \Delta\nu$. The system of equations becomes:

$$\frac{d\nu_i'}{d\tau} = -(1+\lambda)\xi_i + \lambda\xi_{3-i} - \varphi(\nu_i' - \Delta\nu),$$
$$\frac{d\xi_i}{d\tau} = \nu_i' - \nu_d'. \tag{1.3}$$

1.2 Electronic analog for the motion of two blocks

In order to analyze the properties of the BK model, it is possible to build an electronic circuit which differential equations are the same as Eqs. 1.3. The first implementation was done by Field, Venturi and Nori [4] by drawing a direct parallelism between mechanical and electrical quantities. The idea was to use capacitance as mass, inductance as the reciprocal of elastic constant, voltage as velocity and current as position. However, this implementation has two main drawbacks. The first one is the usage of inductances, which are typically bulky and have intrinsically large tolerances compared with other components, resulting in higher uncertainties; moreover, their tunability is very low. The second issue is that the current is a state variable, and it is less straightforward to measure it with respect to voltage.

It is possible to use another implementation [3] which does not rely on inductances and uses only voltages as state variables. In order to do so it is necessary to rewrite the system equations as integral equations, so that they can be implemented by electronic integrators that are more stable than the differentiators. The new state variables are defined as $V_i \equiv \nu_i V_0$ and $W_i \equiv \xi_i V_0$ and the new time constant is given by $\tau = RC$, where R and C are suitably chosen resistance and capacitance. Integrating the system of Eqs. 1.3 for a moving surface and replacing $V_i' \equiv V_i + \Delta V$ and $V_d' \equiv V_d + \Delta V$, where $V_d \equiv V_0\nu_d$ and $\Delta V \equiv V_0\Delta\nu$, leads to the following system of equations:

$$V_i + \Delta V = -\frac{1}{RC} \int \left[(1+\lambda)W_i - \lambda W_{3-i} + V_0 \varphi \left(\frac{V_i}{V_0} \right) \right] \mathrm{d}t,$$

$$(1.4)$$

$$W_i = -\frac{1}{RC} \int (V_d - V_i)\, \mathrm{d}t,$$

where $\lambda = R/R_c$ and R_c is a suitably chosen resistance.

These differential equations are implemented by the circuit shown in Fig. 1.3, which makes use of resistors, capacitors, diodes and operational amplifiers, without any inductance. Assuming for a while that ΔV and the nonlinear element $\varphi(V_i/V_0)$ were not present, the two integrations above could be promptly implemented by considering the black part of the circuit diagram.
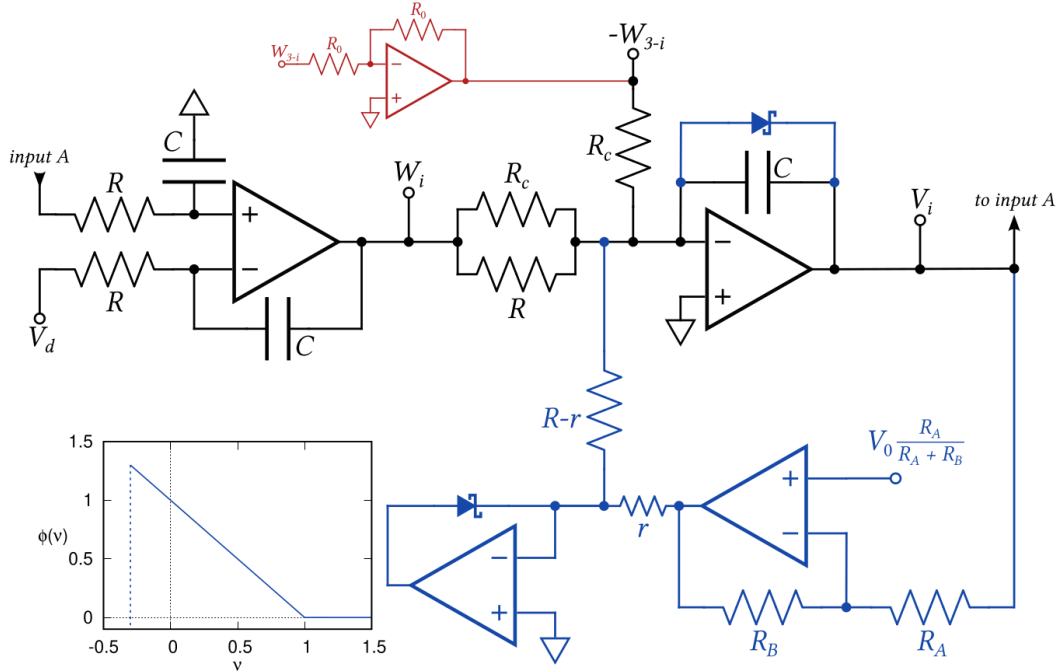

Figure 1.3: Inductorless representation of the BK model. The circuit diagram refers to a single block, labeled by $i = 1, 2$. The bottom left plot shows the characteristic of the nonlinear element, i.e. the blue part of the diagram. The red part is a standard inverting operational amplifier, which is necessary for the coupling between two blocks. Figure adapted from Ref. [3].

The nonlinear term is instead represented by the blue part of the diagram and it is implemented as follows. A Schottky diode is inserted on the feedback network on the integrator producing V_i; this ensures that V_i does not drop below $-V_{\mathrm{diode}}$, where $V_{\mathrm{diode}} \approx 0.3$ V. In order to not contradict the constraint that the "velocity" must be always non-negative, it is necessary to set $\Delta V = V_{\mathrm{diode}}$. In this way the first of the constraints set in Sec. 1.1.2, i.e. $\varphi(V_i < 0) = 0$ is satisfied, since the voltage cannot drop below zero.

The nonlinear friction element consists in a linear drop for the analog of the velocity-weakening force, and it is implemented using two additional op-amps as

follows. The output of the first op-amp is given by $V_0 - V_i R_B / R_A$. Downstream of the resistor r, this voltage is prevented to drop below zero by an active clamp made of the second op-amp which has a diode in its feedback network. The resulting voltage is fed back into the integrator generating V_i through an additional resistor $R - r$.

1.3 Characterization of the single block behavior

With the aim of analyzing the circuit represented in Fig. 1.3, it is necessary to characterize its behavior. The first characterization concerns the function of a single block, in the absence of couplings. In this case $\lambda = 0$ and the differential equations of the system can be simplified as (the subscript i is omitted):

$$\frac{\mathrm{d}^2 V}{\mathrm{d}t^2} + \frac{1}{\tau}\varphi'\left(\frac{V}{V_0}\right)\frac{\mathrm{d}V}{\mathrm{d}t} + \frac{1}{\tau^2}(V - V_d) = 0$$

$$\frac{\mathrm{d}W}{\mathrm{d}t} = \frac{1}{\tau}(V - V_d)$$

(1.5)

where φ' is the derivative of the friction with respect to the velocity V. The equation for the velocity is of the kind met in the classical description of stick-slip vibrations [5], i.e. of the self-sustained oscillations induced by friction. This means that an oscillating behavior for V and W has to be expected.

In order to check the validity of these equations, the circuit was physically implemented in two different manners. The first implementation was done on a breadboard using large electronic components; the main issue with this system is that it is not scalable, due to the fact that a single circuit occupies half of the entire space on the breadboard. The second one consists instead in an integrated board in which 25 circuits like the one in Fig. 1.3 were implemented; the scalability issue is solved in this case, so that this board could be utilized to study the behavior of many coupled blocks, as will be done in the next chapters.

1.3.1 Breadboard implementation

The breadboard implementation was made using 1N5817 Schottky diodes and OP27 op-amps; these op-amps were supplied with $V_{CC} = \pm 12$ V. The nominal values for the resistances and capacitors are $R = R_c = 10$ kΩ, $R_A = R_B = 10$ kΩ, $r = 1.8$ kΩ and $C = 100$ nF, so that the characteristic time of the circuit is $\tau = 1$ ms. The input voltages are $V_0 = 1$ V and the variable voltage V_d, while the output voltages are V and W (the subscript i is omitted).

The single block behavior of this circuit is shown in Fig. 1.4. As expected by Eqs. 1.5, both the velocity V and the position W exhibit an oscillating behavior. While W closely resembles a sinusoidal wave, V possesses a lower clamping that makes it different from a simple wave; this clamping is due to the presence of the Schottky diodes, which prevent that the velocity becomes negative, as discussed in Sec. 1.2. In the end, both the frequency and the amplitude of the waves depend on the driving voltage V_d.
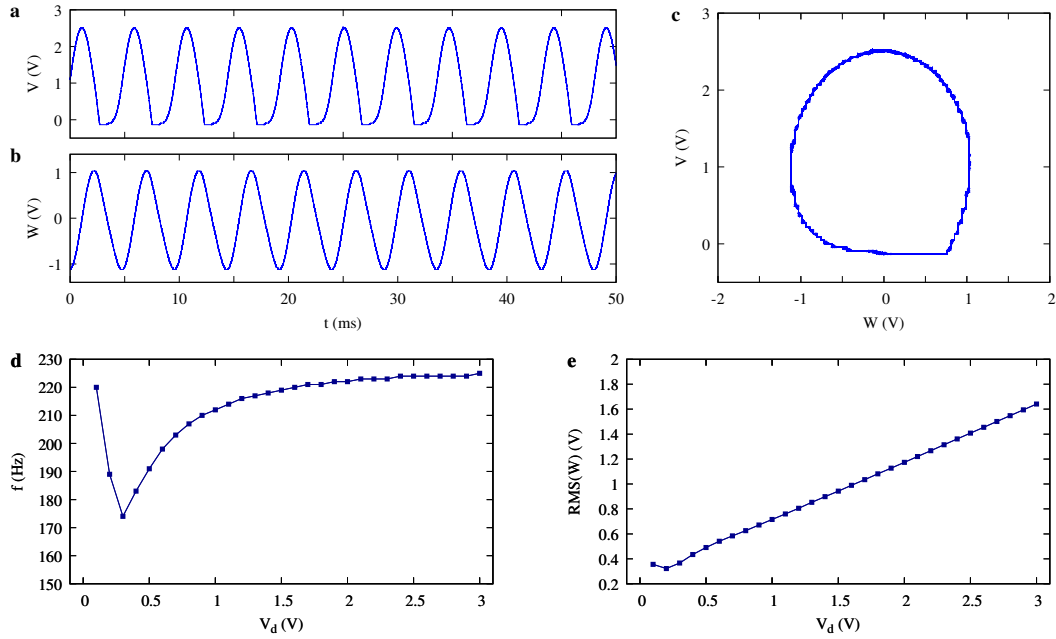
Figure 1.4: Oscillating behavior for the circuit implemented on the breadboard. (a) Plot of W and (b) of V as a function of time, for $V_d = 1$ V. (c) Phase portrait (Lissajous figure) of V versus W. (d) Frequency and (e) root mean square amplitude of the output signal W as a function of the parameter V_d.

1.3.2   Integrated board implementation

The circuit diagram for each of the 25 chips on the integrated board is equivalent to the one shown in Fig. 1.3. The only differences with the breadboard implementation concern the nonlinear components, i.e. the use of DFLS1100 Schottky diodes and quad operational amplifiers OP470, which should offer comparable performances to the components used in the previous section, i.e. 1N5817 Schottky diodes and OP27 op-amps.

A comparison between the single block behavior of this circuit and the one implemented in the previous section is shown in Fig. 1.5. The most notable difference is the amplitude of the waveforms and of the Lissajous figures, which is higher in the integrated board case. Another discrepancy between the two plots lies in the frequency behavior at low driving voltage V_d, i.e. the initial "drop" in the frequency is more pronounced in the breadboard case with respect to the integrated circuit. These distinctions are all probably due to the different diodes and op-amps utilized in the two cases, but they do not modify the actual dynamics of the circuit.

Despite being slightly different, both implementations comply with the oscillating behavior predicted by Eqs. 1.5. It is thus reasonable to assume that both the integrated circuit and the one on the breadboard can potentially be a consistent physical implementation of the BK model. In order to furtherly strenghten this hypothesis, an analysis on the behavior of two coupled blocks will be carried out in the next section. From now on, only the integrated board implementation will be considered, due to the scalability issues that were discussed beforehand.
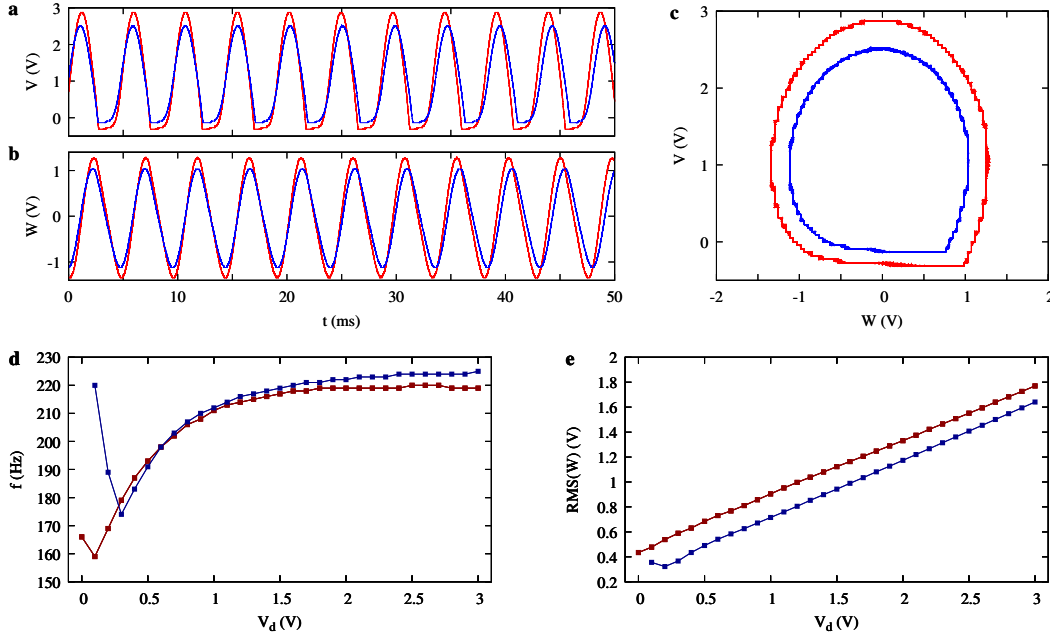
Figure 1.5: Oscillating behavior for the circuit implemented on the integrated board (red) and the one implemented on the breadboard (blue). (a) Plot of W and (b) of V as a function of time, for $V_d = 1$ V. (c) Phase portrait (Lissajous figure) of V versus W. (d) Frequency and (e) root mean square amplitude of the output signal W as a function of the parameter V_d.

1.4   Characterization of the double block behavior

The coupling between two blocks is performed by connecting the inverted voltage $-W_2$ of the second block to the inverting input of the op-amp generating V_1 on the first block (see Fig. 1.3), and viceversa, in order to comply with Eqs. 1.4.

The behavior of the two coupled blocks is shown in Fig. 1.6. By looking at the waveforms $V_i(t)$ and $W_i(t)$ it is possible to notice that the simple periodic behavior is no longer observed. Furthermore, the Lissajous figures do not show a stationary orbit like the single block case. This hints that the dynamics in the presence of coupling might be chaotic, i.e. deterministic but unpredictable, and surely non-periodic.

Another way to check the presence of chaos in the system is to make use of a bifurcation diagram, i.e. the distribution of the local maxima of a state variable (position, velocity) as a function of an external parameter (driving force). This diagram is shown in Fig. 1.7 for the position W_1 (W_2 behaves similarly) as a function of V_d. The scan of the V_d parameter was carried out by switching off the circuit's power supply, changing the voltage V_d, and the switching the power supply back on. This ensured that the recorded evolution was independent of the previous state. It is possible to notice that the dynamics is richer for $V_d \lesssim 0.1$ V, where several maxima can be detected. In contrast, for $V_d \gtrsim 0.1$ V, only one maximum can be observed; in this regime the system behaves similarly to the single block case, manifesting periodic sinusoidal-like oscillations.
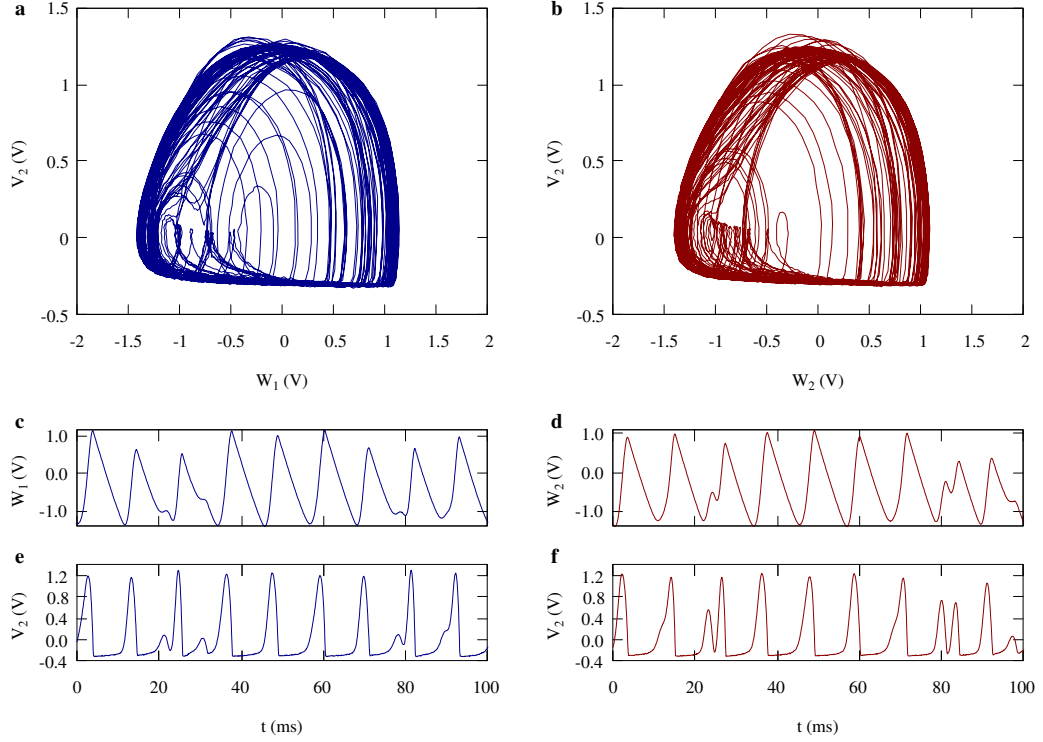
Figure 1.6: Chaotic behavior of two coupled blocks for $V_d = 0.05$ V. Phase portraits of V_i vs W_i for the first (a) and second (b) block, for a total time of 1 s. Time series plots for W_1 (c), V_1 (e), W_2 (d) and V_2 (f), for a total time of 100 ms.
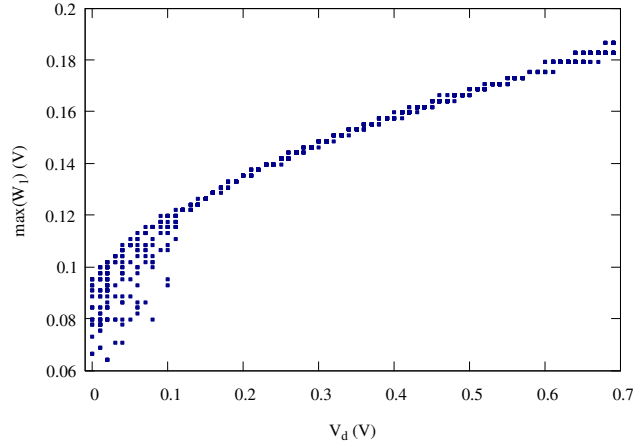

Figure 1.7: Bifurcation diagram for two coupled blocks. The local maxima of W_1 are plotted as a function of the external parameter V_d, which is varied in steps of 10 mV.

It is therefore safe to assume that, for low driving voltages V_d, the coupled system of two blocks shows a chaotic behavior. The reason why this does not occur at higher voltages might be that the driving force is so strong that the blocks behave independently of it. Nonetheless, these analyses are not enough to say that this circuit is actually a chaotic system. In order to prove this statement, a deeper chaos analysis is carried out in the next chapter.

Chapter 2

Chaos analysis of multiple coupled blocks

2.1 Two blocks
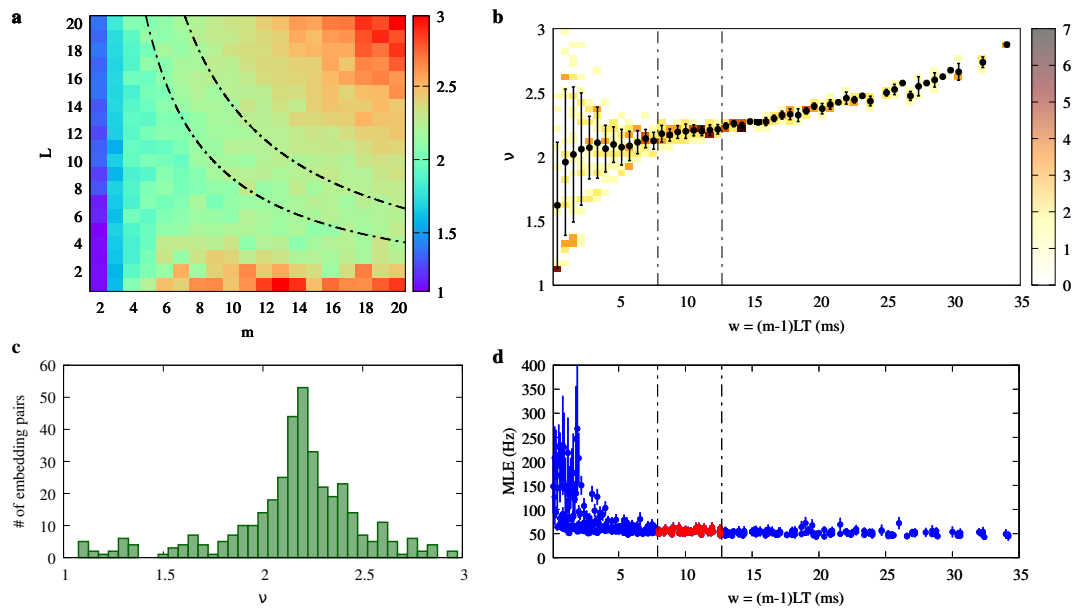
Figure 2.1: Edge

2.2   Three blocks
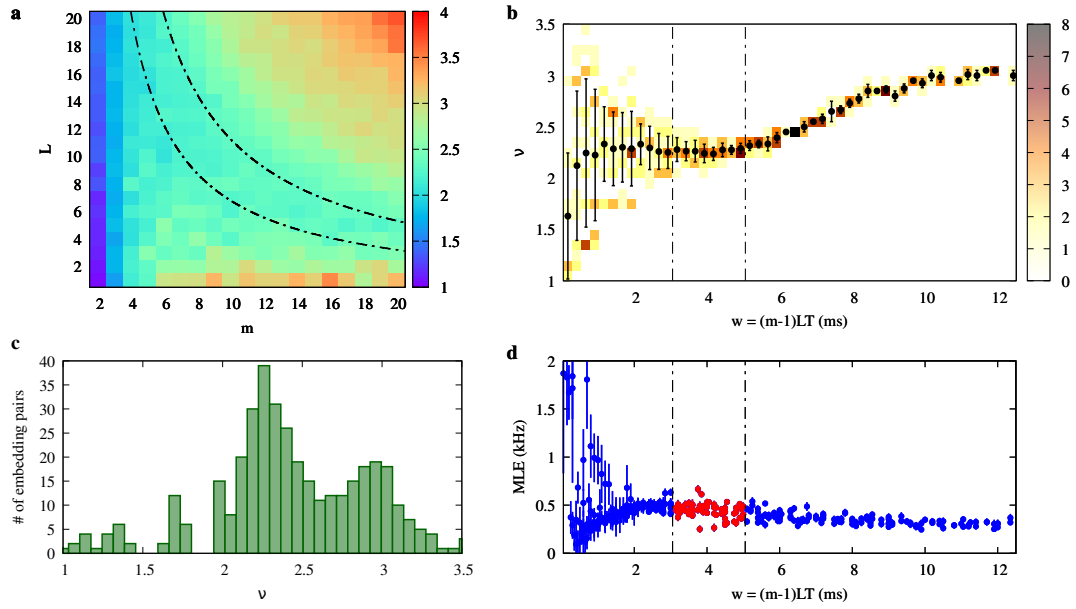
Figure 2.2: Edge
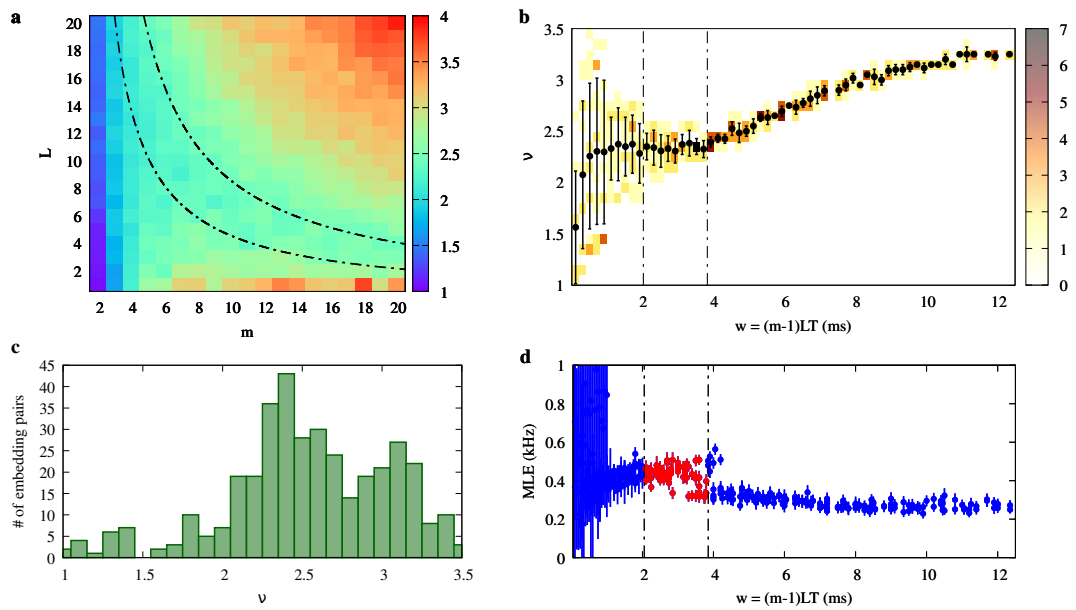
Figure 2.3: Middle

2.3 Four blocks
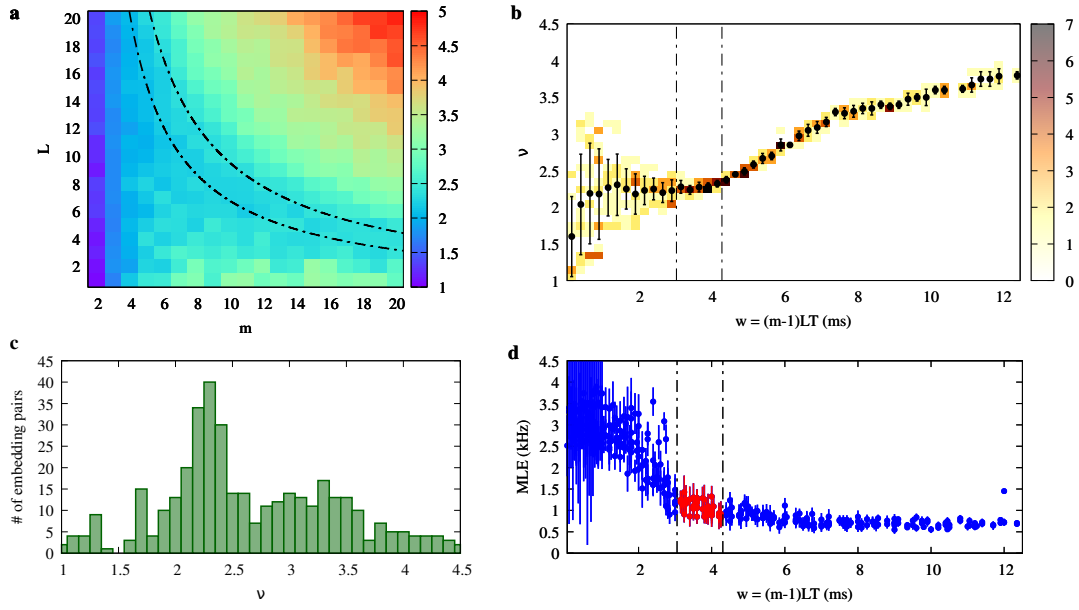
Figure 2.4: Edge

2.4 Five blocks
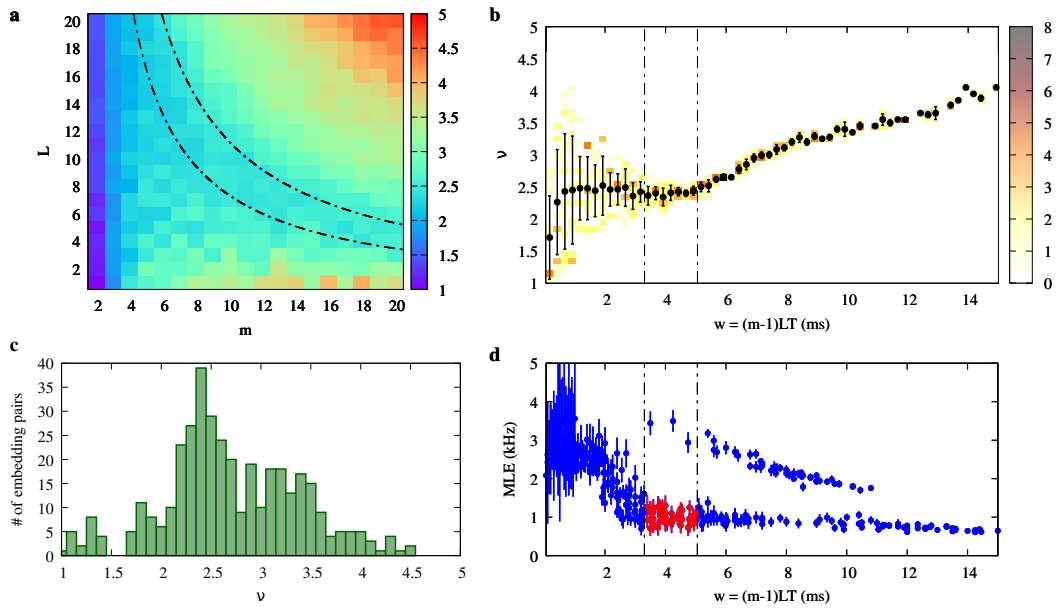
Figure 2.5: Edge
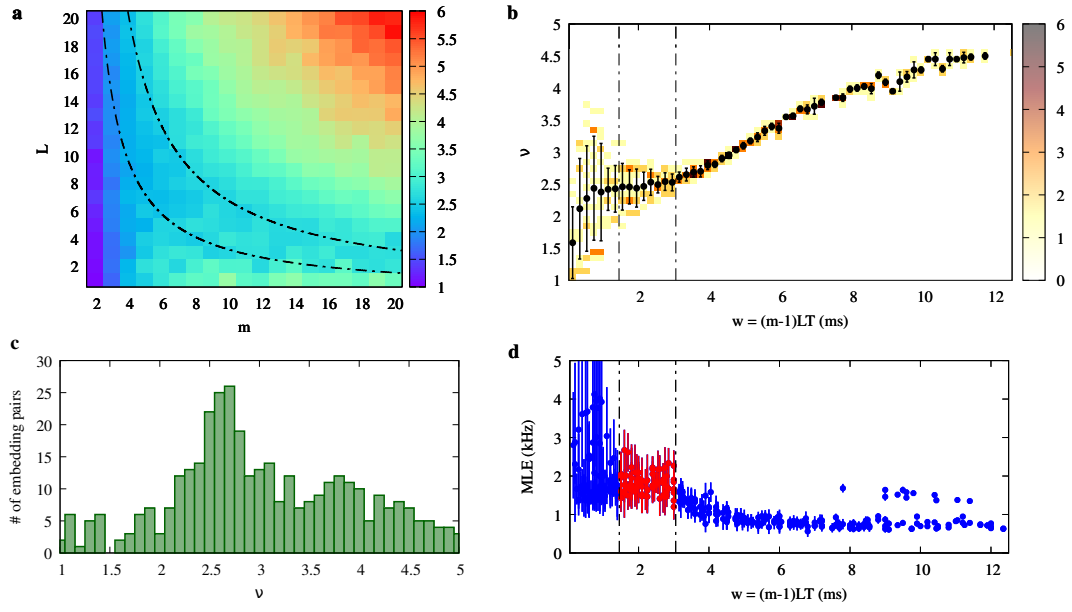
Figure 2.6: Middle

2.5   Six blocks
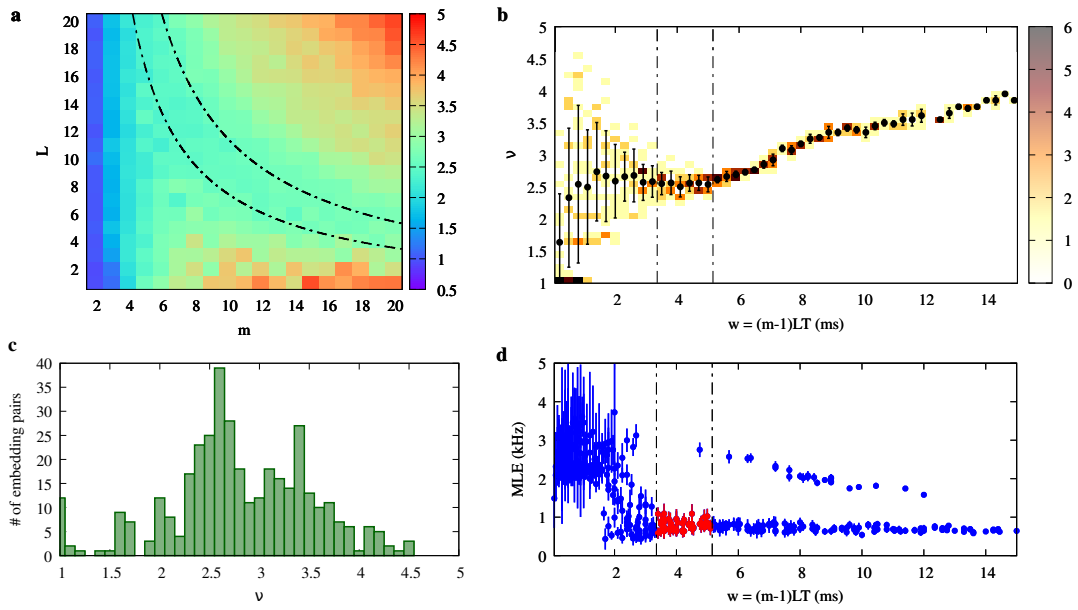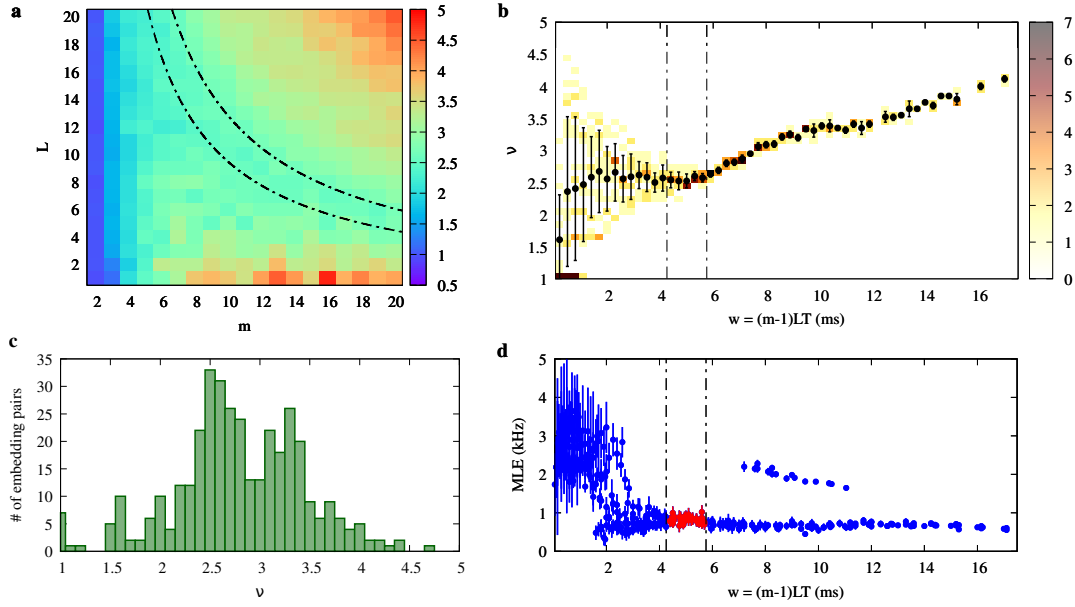

Figure 2.7: Edge
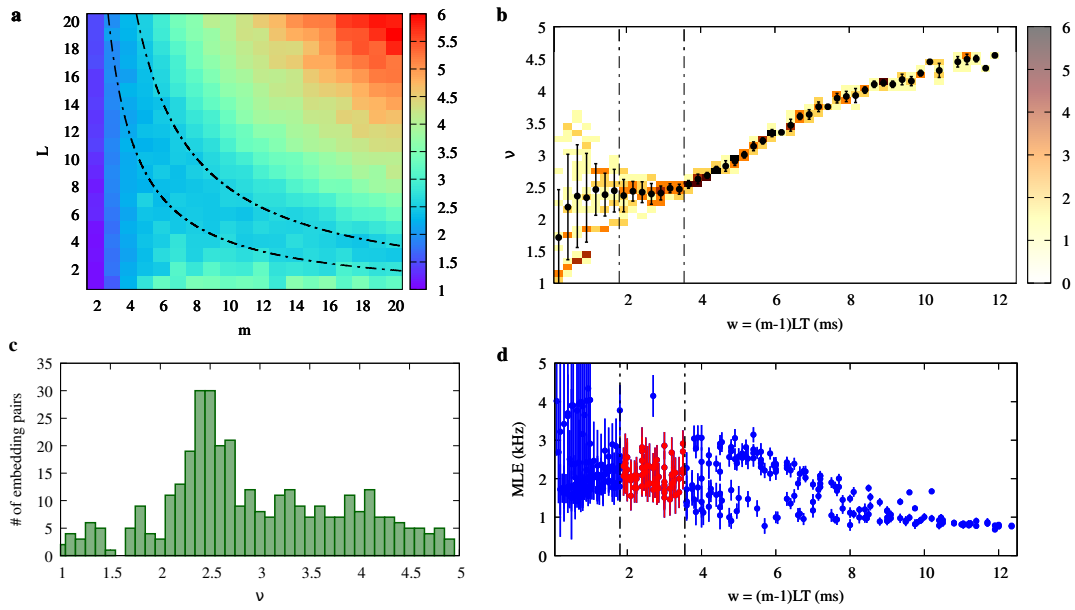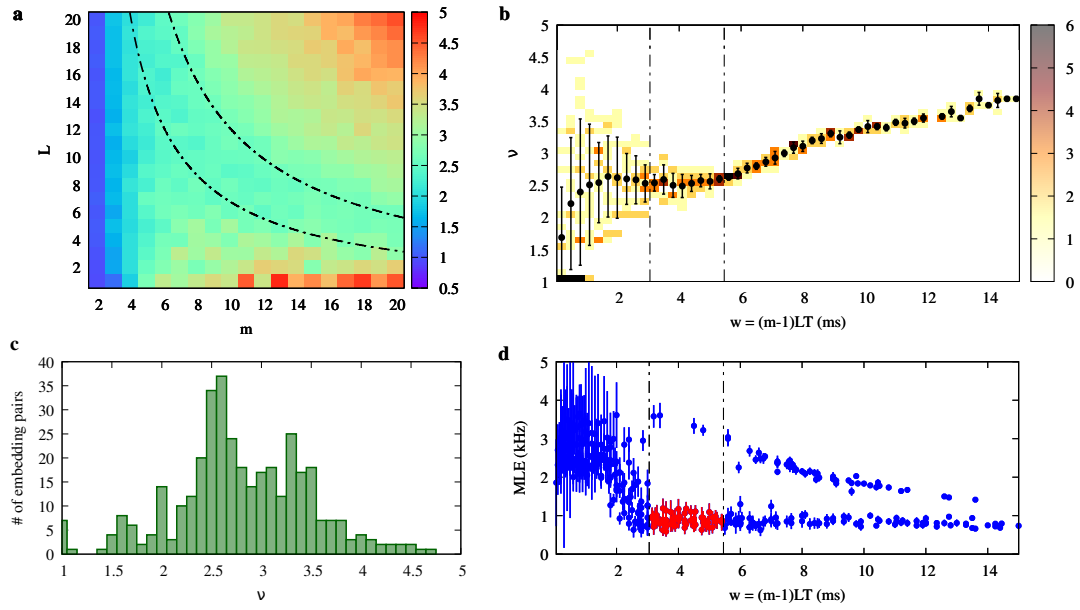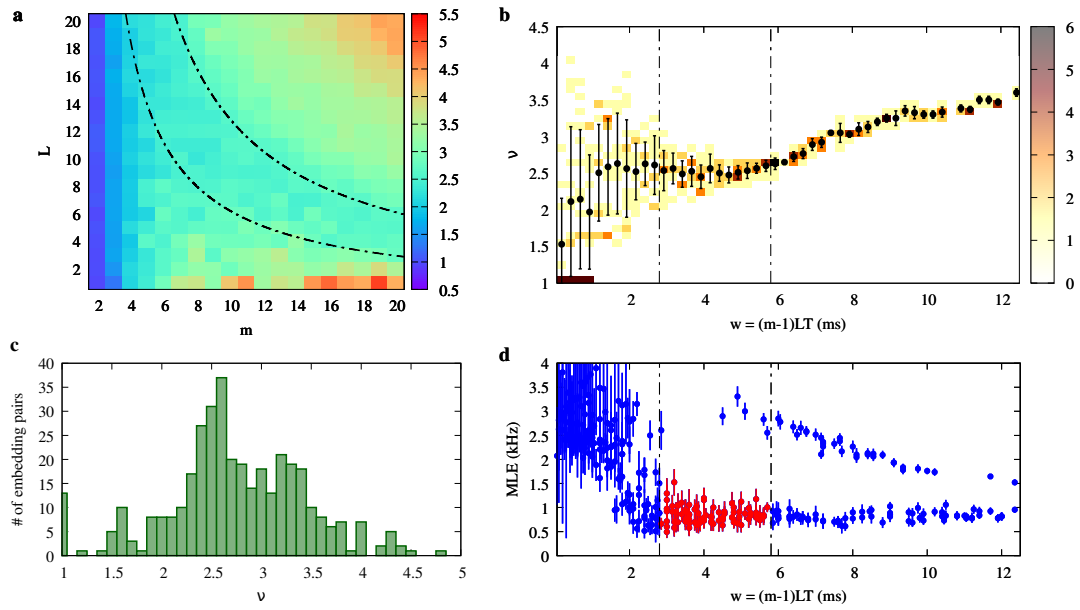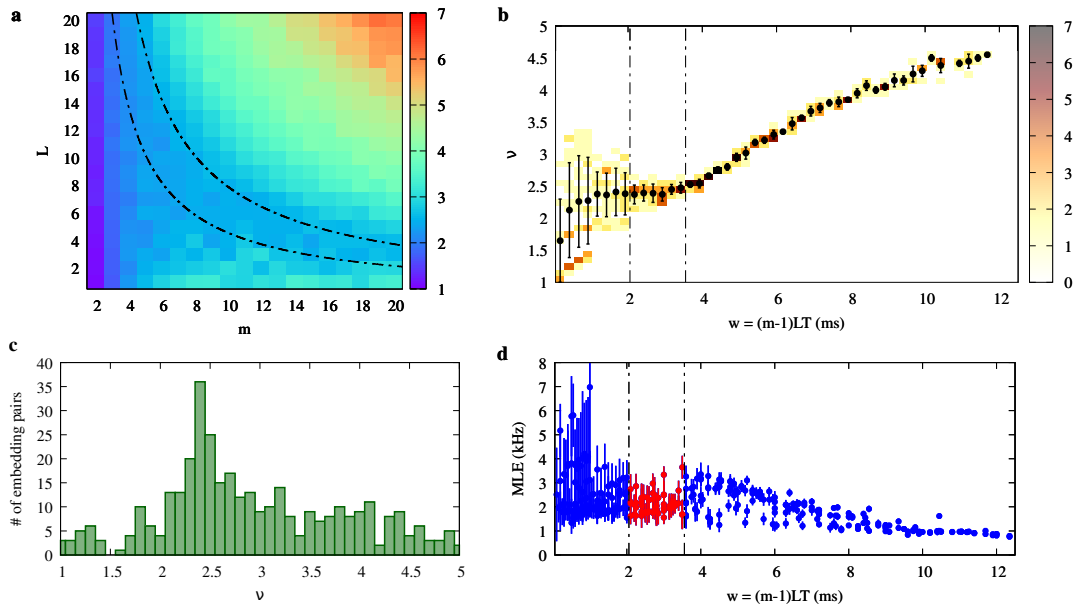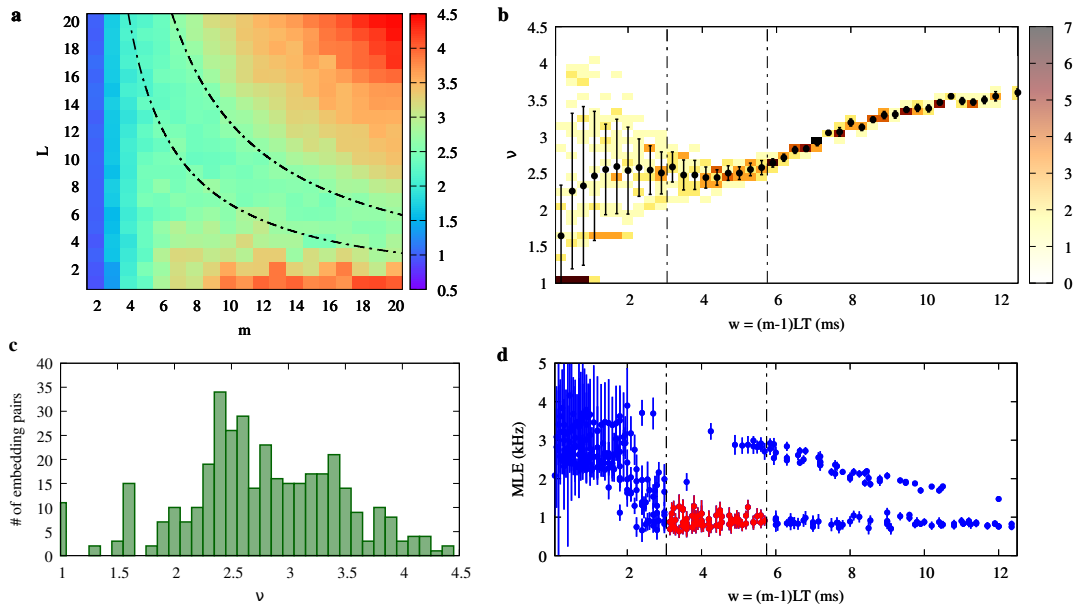
2.6   Seven blocks

Figure 2.8: Edge

Figure 2.9: Middle

2.7 Eight blocks

Figure 2.10: Edge

2.8 Nine blocks

Figure 2.11: Edge

Figure 2.12: Middle

2.9   Ten blocks

Figure 2.13: Edge

2.10   Fifteen blocks
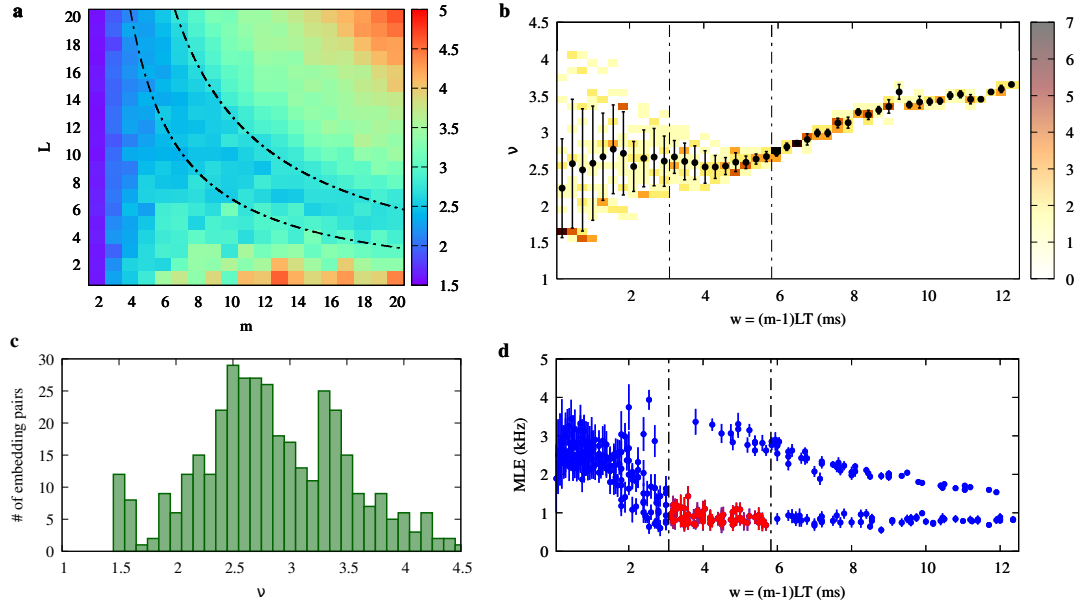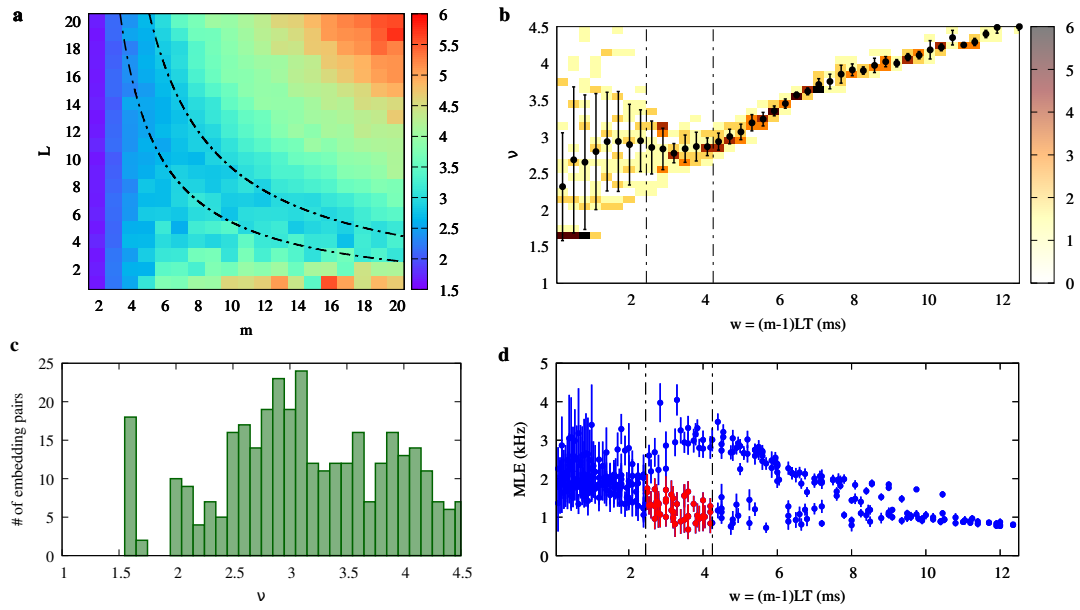

Figure 2.14: Edge

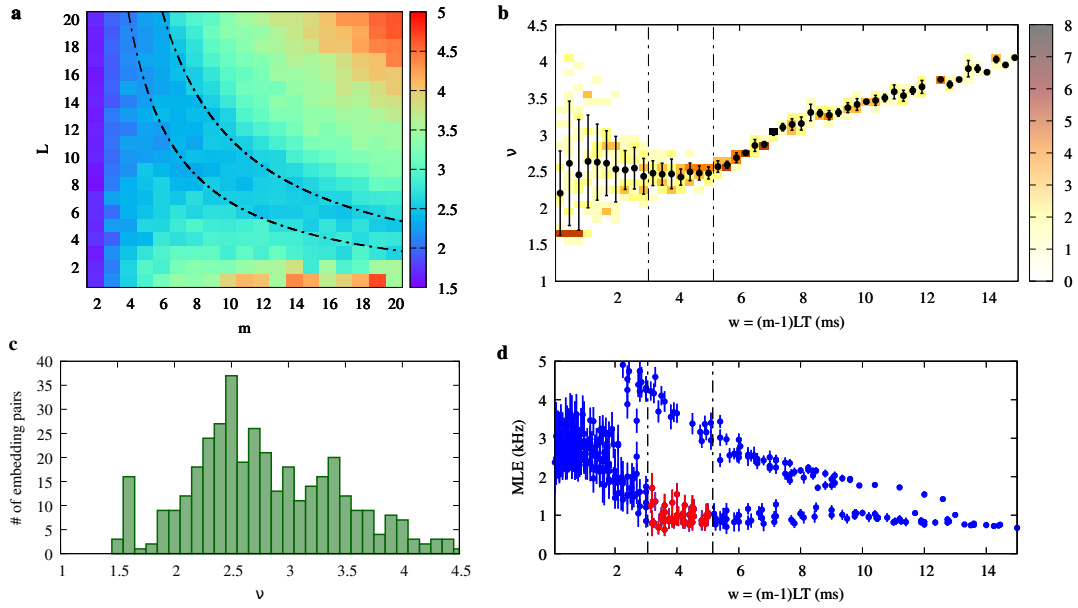Figure 2.15: Middle

2.11   Twenty blocks

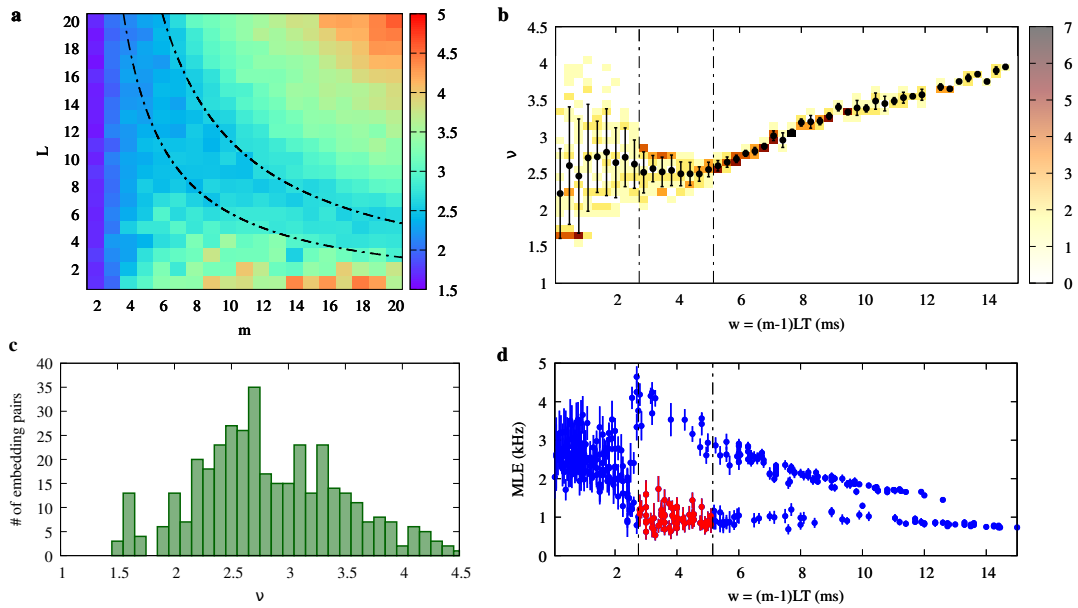

Figure 2.16: Edge

2.12   Twentyfive blocks
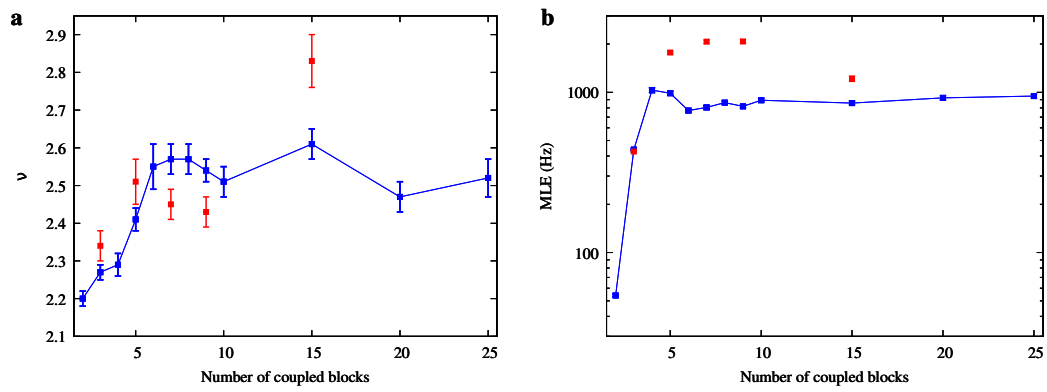

Figure 2.17: Edge

2.13   Conclusions

Figure 2.18: Edge (blue) and middle (red)

Chapter 3

Earthquake simulation

Bibliography

[1] R. Burridge and L. Knopoff. "Model and theoretical seismicity". In: *Bulletin of the Seismological Society of America* (1967).

[2] Zeev Olami, Hans Jacob S. Feder, and Kim Christensen. "Self-organized criticality in a continuous, nonconservative cellular automaton modeling earthquakes". In: *Phys. Rev. Lett. 68, 1244* (1992).

[3] A. Perinelli, R. Iuppa, and L. Ricci. "A scalable electronic analog of the Burridge–Knopoff model of earthquake faults". In: *Chaos 33, 093103* (2023).

[4] S. Field, N. Venturi, and F. Nori. "Marginal Stability and Chaos in Coupled Faults Modeled by Nonlinear Circuits". In: *Phys. Rev. Lett. 74* (1995).

[5] K. Popp and P. Stelter. "Stick-slip vibrations and chaos". In: *Philos. Trans. Roy. Soc. A* (1990).